Original Article

trd Tuberculosis & Respiratory Diseases

Single-Cell Analysis Identifies Factors Associated with Rheumatoid Arthritis-Related Interstitial Lung Disease in Comparison with Idiopathic Pulmonary Fibrosis

Dongjun Kim[1,2]*, Hyun Lee[3]*, Sang-Heon Kim[3], Yeonghee Eun[4], Hyun Je Kim[1,2,5] and Bo-Guen Kim[6]

[1]Department of Biomedical Sciences, Seoul National University Graduate School, Seoul, [2]Cancer Research Institute, Seoul National University College of Medicine, Seoul, [3]Department of Internal Medicine, Hanyang University College of Medicine, Seoul, [4]Division of Rheumatology, Department of Internal Medicine, Kangbuk Samsung Hospital, Sungkyunkwan University School of Medicine, Seoul, [5]Department of Microbiology and Immunology, Seoul National University College of Medicine, Seoul, [6]Division of Pulmonary Medicine, Department of Internal Medicine, Kangbuk Samsung Hospital, Sungkyunkwan University School of Medicine, Seoul, Republic of Korea

https://doi.org/10.4046/trd.2026.0085
ISSN: 1738-3536(Print)/
2005-6184(Online)
Tuberc Respir Dis 2026;89:542-552

Check for updates

Copyright © 2026 The Korean Academy of Tuberculosis and Respiratory Diseases

Address for correspondence
Hyun Je Kim
Department of Microbiology and Immunology, Seoul National University College of Medicine, 103 Daehak-ro, Jongno-gu, Seoul 03080, Republic of Korea
Phone 82-2-740-8307
E-mail hjkim0518@gmail.com
Address for correspondence
Bo-Guen Kim
Division of Pulmonary Medicine, Department of Internal Medicine, Kangbuk Samsung Hospital, Sungkyunkwan University School of Medicine, 29 Saemunan-ro, Jongno-gu, Seoul 03181, Republic of Korea
E-mail kbg1q2w3e@gmail.com

Received Apr. 28, 2026
Revised Jul. 14, 2026
Accepted Jul. 25, 2026
Published online Jul. 28, 2026

*These authors contributed equally to the manuscript as first author.

It is identical to the Creative Commons Attribution Non-Commercial License (http://creativecommons.org/licenses/by-nc/4.0/).

Abstract

Background: Interstitial lung disease (ILD) is a common but serious extra-articular manifestation of rheumatoid arthritis (RA). RA-associated ILD (RA-ILD), which often presents with the usual interstitial pneumonia pattern, can resemble idiopathic pulmonary fibrosis (IPF), though the treatment and progression of these two conditions differ. However, the immunologic and molecular mechanisms associated with RA-ILD and IPF development have not been well elucidated at the single-cell level.

Methods: To investigate the underlying mechanisms associated with RA-ILD and IPF development, we performed single-cell RNA sequencing (scRNA-seq) of peripheral blood mononuclear cells (PBMCs) from five RA-ILD patients and five patients with IPF with a matched age and sex distribution.

Results: A high-quality scRNA-seq dataset comprising 31,416 peripheral immune cells was generated. Overall immune composition was similar between groups; however, a significant elevation of natural killer (NK) cells was seen among the RA-ILD PBMCs, with increased expression of cytotoxic and inflammation-related genes (*GZMB*, *GZMH*, *PRF1*) as well as interferon-related genes (*STAT1*, *STAT3*, *IRF9*, *IFNG*). Myeloid subsets displayed distinct transcriptional programs in IPF and RA-ILD: IPF $CD16^+$ monocytes were enriched for transforming growth factor beta (TGF-β)–driven fibrotic signaling, whereas RA-ILD monocytes exhibited type I/II interferon pathway activation. Fibrosis-related genes (*TGFB1*, *SMAD3*, *SMAD7*, *TGIF1*) were specifically upregulated in IPF.

Conclusion: RA-ILD and IPF share similar peripheral immune cell compositions, but exhibit distinct transcriptional activation patterns. RA-ILD is characterized by increased NK-cell–driven cytotoxic and interferon-related responses, along with interferon-activated monocytes. In contrast, IPF shows a TGF-β–dominant fibrotic program, with transcriptional activation of $CD16^+$ monocytes and upregulation of fibrosis-related genes.

Keywords: Rheumatoid Arthritis-Associated Interstitial Lung Disease; Idiopathic Pulmonary Fibrosis; Single-Cell Sequencing

Introduction

Rheumatoid arthritis (RA) is one of the most common rheumatic diseases and is primarily characterized by joint involvement. However, a considerable proportion of patients with RA exhibit pulmonary manifestations[1-3]; among these, interstitial lung disease (ILD) is a common and serious manifestation involving the lungs[3]. The risk of developing ILD is higher in patients with RA than those without[2], and the occurrence of ILD in RA is associated with higher mortality than its absence[4-6]. Moreover, the development of ILD in RA is linked to reduced quality of life, impaired physical function, and increased healthcare costs[7,8].

Despite its clinical importance, the heterogeneity and variability in the onset and prognosis of RA-associated ILD (RA-ILD) make diagnosis and treatment challenging. Recently, single-cell sequencing technology, which enables multidimensional profiling of individual cells, has been applied in various fields. In RA-related diseases, this approach has facilitated the identification of cell subtypes, discovery of molecular functions, and elucidation of novel pathways[9-15]. However, previous single-cell sequencing studies in RA have primarily compared RA patients with healthy controls and focused on synovial tissue from affected joints[12-15]. While single-cell sequencing studies have been conducted in ILD, they have been limited to idiopathic pulmonary fibrosis (IPF) and systemic sclerosis-associated ILD. There is still insufficient single-cell sequencing data for RA patients stratified by ILD status.

Among RA-ILD, the usual interstitial pneumonia (UIP) pattern is the most common[16]. Although this pattern resembles that of IPF, which lacks an identifiable cause, the two conditions differ in disease course, treatment, and underlying pathogenesis. Nevertheless, they are often difficult to distinguish at the time of initial clinical evaluation[17]. To date, no studies have directly compared disease-related factors between IPF and RA-ILD with a UIP pattern, and we therefore aimed to conduct such an analysis. By comparing single-cell RNA sequencing (scRNA-seq) data between patients with RA-ILD with a UIP pattern and those with IPF, we aimed to identify gene-expression differences and elucidate factors associated with the development of RA-ILD.

Materials and Methods

1. Study populations

Study subjects were recruited from two tertiary general hospitals from February 1, 2024, to May 31, 2025. Participants were eligible for inclusion if they were adults aged 19 years or older with a confirmed diagnosis of IPF, or adults aged 19 years or older who had been diagnosed with RA by a board-certified rheumatologist, assigned an RA-related diagnostic code, and subsequently evaluated by a pulmonologist for the presence of RA-ILD. Among the latter, only individuals whose imaging studies were interpreted by a board-certified radiologist as demonstrating a UIP pattern were included. The study aimed to enroll RA-ILD patients with a UIP pattern (n=5) and IPF patients (n=5) in a 1:1 ratio matched by age and sex.

Individuals were excluded if they declined participation; had uncontrolled, severe respiratory comorbidities unrelated to ILD, such as tuberculous-destroyed lungs, bronchiectasis not associated with ILD, severe asthma, or chronic obstructive pulmonary disease; had psychiatric disorders that could interfere with study participation, including schizophrenia; or had severe systemic illnesses such as chronic kidney disease requiring dialysis, advanced liver disease, significant cardiac disease, or active malignancy.

The study protocol was approved by the Institutional Review Boards of Hanyang University Hospital (No. HYUH 2023-09-014) and Kangbuk Samsung Hospital (No. KBSMC 2024-12-024). All participants provided written informed consent prior to enrolment in the study.

2. Sample collection

For single-cell sequencing, peripheral blood was drawn into CPT tubes (BD Vacutainer® CPT – 36276, BD, Franklin Lakes, NJ), with a total volume of 10 mL collected for peripheral blood mononuclear cell (PBMC) isolation. After centrifugation, the upper layer (PBMC-containing fraction) was equally divided into two separate tubes. The PBMC fractions from both tubes were then pooled and transferred into a new conical tube, and the total volume was adjusted to 15 mL. The cells then underwent multiple washing steps, after which the pelleted PBMCs were resuspended in freezing media and aliquoted into two vials. Following initial cooling at −20°C and subsequent storage at −80°C, the samples were ultimately transferred to a liquid nitrogen tank until use in downstream experiments[18].

For each participant, blood samples were collected simultaneously for single-cell sequencing analysis and for measurement of rheumatoid factor, anti-cyclic citrullinated peptide antibodies, erythrocyte sedimentation rate (ESR), and C-reactive protein (CRP).

3. Single-cell preparation and sequencing

A volume of cell suspension containing 4,000 cells per

patient was calculated using an automatic cell counter (LUNA-FL, Logos Biosystems, Gunpo, Korea). Cells from five individuals were pooled to generate a single gel-bead in emulsion (GEM). Each GEM contained a sample from both sexes. GEM generation and library construction were performed using the Chromium Next GEM single cell 3' Reagent Kit v4 according to the manufacturer's instructions (document CG000731, 10X Genomics, Pleasanton, CA, USA). GEMs and cDNA were generated using Chromium GEM-X single cell 3' Kit v4 (10X Genomics, PN-1000693). Libraries were constructed using cDNA and made using the Library Construction Kit C (10X Genomics, PN-1000694). The size distribution and concentration of the resulting gene expression (GEX) libraries were assessed using a TapeStation 4200 (Agilent, Santa Clara, CA, USA), and then the GEX libraries were sequenced using the Illumina NovaSeq 6000 platform (San Diego, CA, USA).

4. Genomic DNA extraction and genotype-based demultiplexing

Genomic DNA (gDNA) was extracted from PBMCs of each patient using the QIAamp DNA Mini Kit (Qiagen, Hilden, Germany). The quality and quantity of gDNA were measured using a NanoDrop One spectrophotometer (Thermo Fisher Scientific, Waltham, MA, USA). Variant calling was performed for each individual using gDNA aligned to the hg19 reference genome. Using variant call format data, pooled single-cell data were demultiplexed based on single-nucleotide polymorphism differences using the demuxlet tool.

5. scRNA-seq data processing, cell clustering, and dimension reduction

Cell Ranger version 8.0.1 was used to align the FASTQ files with the GRCh38 reference genome (10X Genomics) and to generate count matrices. Analyses were performed using Seurat (v5.0.2) and Scanpy (v1.9.8) including quality control, normalization, scaling, dimension reduction, clustering, and visualization. Empty droplets and ambient RNA contamination were removed using SoupX[19] and doublets were identified and removed using scDblFinder[20]. Each sample data point underwent filtration of the expression matrix based on specific criteria, including total unique molecular identifier counts between 750 and 4,000 and mitochondrial gene percentage <5%. The count matrix was normalized using the log method, and the top 2,000 variable genes were collected and used in principal component analysis for dimension reduction. Batch effects across samples were corrected using single-cell variational inference tools (scVI). scVI-integrated latent space was used for the uniform manifold approximation and projection (UMAP). Pathway enrichment analysis was conducted using the Gene Ontology database and gene set enrichment analysis (GSEA). Differentially expressed genes (DEGs) were filtered with the FindMarkers function using a log2 fold change >0.25 and adjusted p-value <0.05. This analysis was applied to all annotated immune cell subsets; the complete results are provided in Supplementary Table S1.

6. Cell-type annotation

Cell-type annotation was performed using CellTypist, a well-established cell-type annotation tool developed by the Teichmann Lab (Cambridge, UK). The Healthy coronavirus disease 2019 (COVID-19) PBMC reference model (version 1) was used, which was trained on PBMCs from both healthy donors and individuals with COVID-19.

7. Statistical analyses

Statistical analyses were performed using R (v4.4.0; R Foundation for Statistical Computing, Vienna, Austria), Python (v3.10; Python Software Foundation, Wilmington, DE, USA), and GraphPad Prism (v8.4.2; GraphPad Software Inc., San Diego, CA, USA). Differential GEX analysis was conducted using the FindMarkers function in Seurat, and the p-value was calculated using the Wilcoxon rank-sum test. For GSEA, genes were ranked based on differential expression statistics (Wilcoxon rank-sum test), and enrichment significance was evaluated using permutation-based testing with false discovery rate correction. Cell-type proportions were calculated across two groups using the Mann-Whitney test.

Results

1. Baseline characteristics

A total of eight patients diagnosed with RA-ILD were initially screened from the seropositive RA cohort. Of these, three patients were excluded due to blood sampling failure (n=1), age mismatch (n=1), and presence of a non-UIP radiologic pattern (non-specific interstitial pneumonia; n=1). The remaining five patients with RA-ILD exhibiting a UIP pattern were selected for single-cell RNA sequencing analysis. To enable comparative transcriptomic profiling, five patients with IPF matched for age and sex distribution were recruited. All IPF patients tested negative for rheumatologic serology, ensuring distinction from autoimmune-associated ILD (Figure 1).

A total of ten patient samples were analyzed, com-

Figure 1. Flowchart of patient selection and categorization. SPRA: seropositive rheumatoid arthritis; RA-ILD: rheumatoid arthritis-associated interstitial lung disease; NSIP: nonspecific interstitial pneumonia; UIP: usual interstitial pneumonia; IPF, idiopathic pulmonary fibrosis.

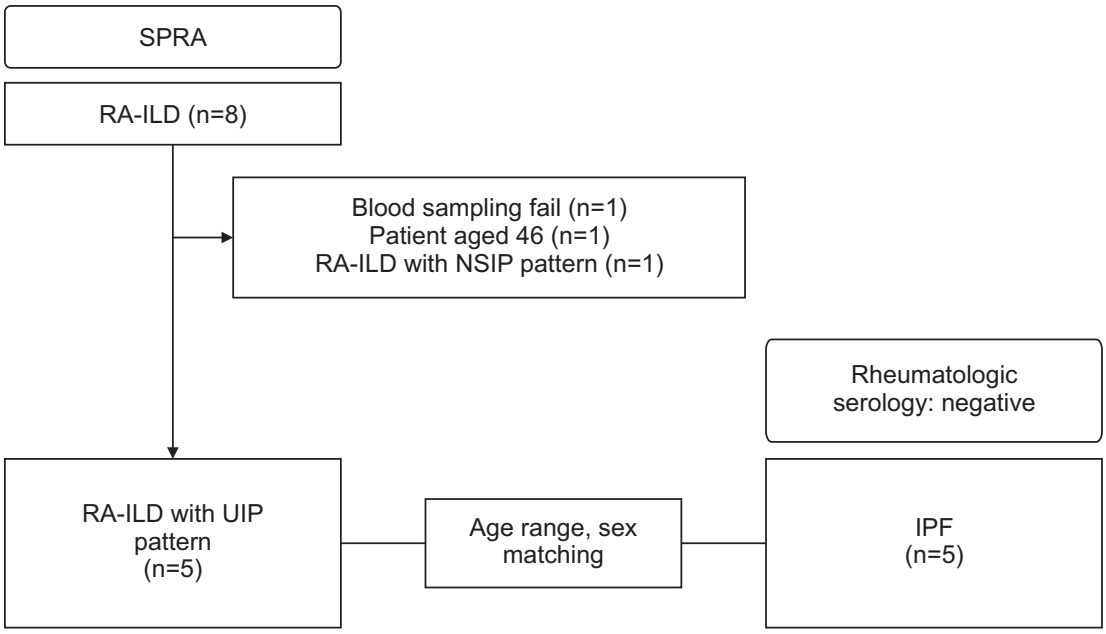

prising two distinct cohorts: RA-ILD and IPF. The RA-ILD group included five individuals (three males and two females) with ages ranging from 55 to 78 years (median age, 72 years). The IPF group also consisted of five individuals (three males and two females), aged between 67 and 78 years (median age, 72 years). Sex distribution was balanced across the two groups. Baseline characteristics and treatment patterns of all participants are summarized in Table 1. The median interval between diagnosis and sequencing was longer in the RA-ILD group (106 months [interquartile range, 65.5 to 153.5]) than in the IPF group (49 months [interquartile range, 32 to 78]). Most patients had a history of prior smoking (three of five in the RA-ILD group and four of five in the IPF group), while the remaining patients in each group had never smoked.

Antifibrotic therapies were assessed. Among RA-ILD cases, pirfenidone was administered in cases 1-1 and 1-5, while nintedanib was used in cases 1-2 and 1-4. Case 1-3 received no antifibrotic treatment. In contrast, all IPF cases (2-1 to 2-5) were uniformly treated with pirfenidone. All RA-ILD cases (1-1 to 1-5) received a combination of methotrexate and prednisolone. No immunosuppressive treatment was administered in any of the IPF cases (2-1 to 2-5).

Clinical parameters were compared between patients with RA-ILD and IPF. The median forced vital capacity (FVC) was higher in the RA-ILD group (2.57 L) than the IPF group (2.00 L), although the percentage predicted FVC value was lower in the RA-ILD group (69.0%) than in the IPF group (78.6%). Similarly, the percentage predicted value of diffusing capacity for carbon monoxide was reduced in both groups, with RA-ILD showing a higher value (61.9%) than IPF (57.0%). Serum Krebs von den Lungen-6 levels were elevated in both cohorts, with IPF patients exhibiting slightly higher levels (722 U/mL) than those with RA-ILD (692 U/mL). Disease Activity Score in 28 Joints was available only for the RA-ILD group, with median values of 3.67 (ESR-based) and 2.56 (CRP-based), indicating moderate disease activity.

2. Comparative PBMC immune profiling

We generated a high-quality scRNA-seq dataset comprising 31,416 cells to characterize peripheral immune cells. The UMAP representation in Figure 2A illustrates the cellular landscape and immune cell types within PBMCs. A total of nineteen distinct clusters were annotated. Cell clusters were annotated using CellTypist, a reference-based annotation tool developed by the Teichmann Lab (Figure 2B). There were no unique cell populations between the IPF and RA-ILD groups, indicating that the overall composition of systemic immune cells was largely comparable between the two groups.

We next examined the proportions of immune cell populations across the two groups (Figure 2C). No marked differences were observed in B cells between

https://doi.org/10.4046/trd.2026.0085

https://e-trd.org/

Table 1. Baseline characteristics of study participants

Sample no.	Age, yr	Sex	Antifibrotic agent	RA medication	FVC, L	FVC, %	DLco, %	KL-6, U/mL	DAS28 (ESR)	DAS28 (CRP)	Diagnosis to sequencing interval, mo*	Smoking history
RA-ILD group												
1-1	63	Male	Pirfenidone	Methotrexate /prednisolone	1.89	40.79	61.91	1,169	4.38	3.42	106	Ex
1-2	55	Female	Nintedanib	Methotrexate /prednisolone	-†	-†	-†	692	2.98	1.98	190	Never
1-3	72	Female	-	Methotrexate /prednisolone	2.84	91.46	68	-‡	3.41	2.31	117	Never
1-4	76	Male	Nintedanib	Methotrexate /prednisolone	2.57	69	48	501	3.92	2.89	58	Ex
1-5	78	Male	Pirfenidone	Methotrexate /prednisolone	-†	-†	-†	-‡	3.67	2.56	73	Ex
					2.57 (1.89–2.84)	69.0 (40.8–91.5)	61.9 (48.0–68.0)	692 (501–1,169)	3.67 (2.98–4.38)	2.56 (1.98–3.42)	106 (65.5–153.5)	
IPF group												
2-1	69	Male	Pirfenidone	-	2.46	93	48.1	964	-	-	39	Ex
2-2	67	Female	Pirfenidone	-	-†	-†	-†	722	-	-	49	Ex
2-3	78	Female	Pirfenidone	-	2	78.59	90.37	-‡	-	-	105	Never
2-4	72	Male	Pirfenidone	-	1.77	46.69	57.03	498	-	-	25	Ex
2-5	75	Male	Pirfenidone	-	-†	-†	-†	-‡	-	-	51	Ex
					2.00 (1.77–2.46)	78.6 (46.7–93.0)	57.0 (48.1–90.4)	722 (498–964)	-	-	49 (32–78)	

Values are presented as median (range), except for the diagnosis to sequencing interval, which is presented as median (interquartile range).
*For patients with RA, the interval was determined by calculating the time from the date of the initial ILD diagnosis to the date of blood sampling. For patients with IPF, the interval was calculated from the date of the initial IPF diagnosis to the blood sampling date. †These patients had no available pulmonary function test results because they failed to undergo the test at the time of blood sampling. ‡KL-6 measurements were unavailable for these patients, as they refused to undergo the assay.
FVC: forced vital capacity; DLco: diffusing capacity of the lung for carbon monoxide; KL-6: Krebs von den Lungen-6; DAS28: disease activity score 28; ESR: erythrocyte sedimentation rate; CRP: C-reactive protein; RA-ILD: rheumatoid arthritis-associated interstitial lung disease; Ex: ex-smoker; IPF: idiopathic pulmonary fibrosis.

Figure 2. (A) Uniform manifold approximation and projection (UMAP) showing immune cell clusters from rheumatoid arthritis-associated interstitial lung disease (RA-ILD) and idiopathic pulmonary fibrosis (IPF) patients. Each dot represents a single cell, colored by cell type. (B) Dot plot showing the expression of marker genes across immune cell types. Dot size indicates the percentage of expressing cells, and color intensity represents scaled average expression. (C) Boxplots showing the proportions of each immune cell population. The following 14 immune cell subsets were compared between the two groups: memory B cells, naive B cells, CD14^{+} monocytes, CD16^{+} monocytes, type 2 conventional dendritic cells (DC2), γδ T cells, mucosal-associated invariant T (MAIT) cells, memory CD4^{+} cytotoxic T cells, natural killer (NK) cells, central memory T cell (Tcm)/naive CD4^{+} T cells, Tcm/naive CD8^{+} T cells, effector memory T cell (Tem)/effector helper T cells, Tem/tissue-resident memory T cell (Trm) CD8^{+} T cells, and regulatory T cells (Tregs). Significant differences were observed in MAIT cells, NK cells, Tcm/naive CD4^{+} T cells, and Tcm/naive CD8^{+} T cells ($p<0.01$), as well as in memory CD4^{+} cytotoxic T cells and Tregs ($p<0.05$). No significant differences were detected in the remaining cell populations. (D) Bar plot showing Hallmark pathways enriched in CD16^{+} monocytes. Pathways enriched in IPF patients are shown in red, whereas those enriched in RA-ILD patients are shown in blue. The transforming growth factor beta (TGF-β) signaling pathway is highlighted with a red box. (E) Gene set enrichment analysis (GSEA) enrichment plot showing the running enrichment score (ES) and the distribution of ranked genes for the Hallmark TGF-β signaling pathway. (F) Heatmap showing pseudobulk gene expression of TGF-β signaling pathway genes in IPF and RA-ILD groups, displayed as z-scores. Mkps: megakaryocyte progenitors; ns: not significant. *$p<0.05$. †$p<0.01$.

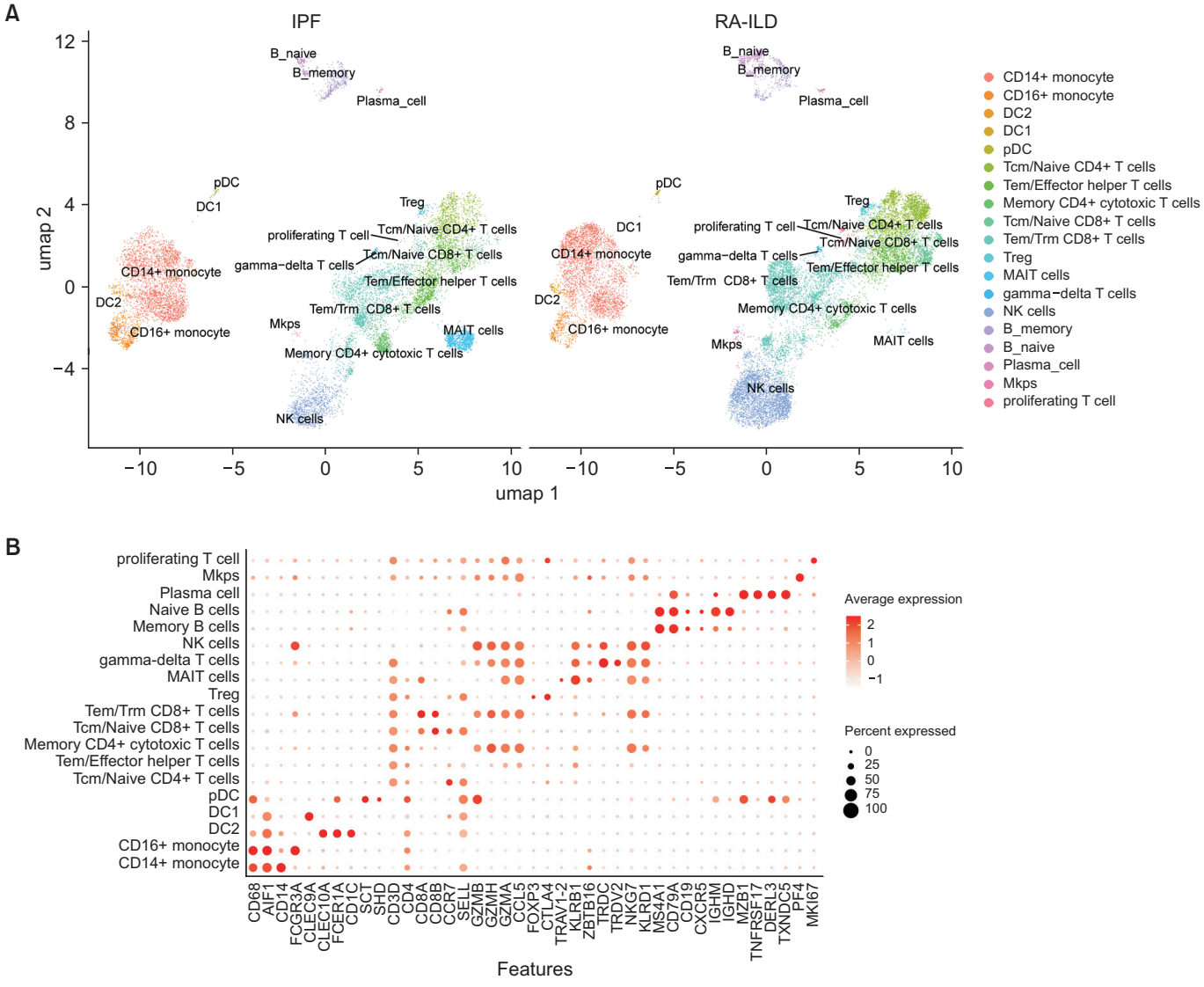

Figure 2. Continued

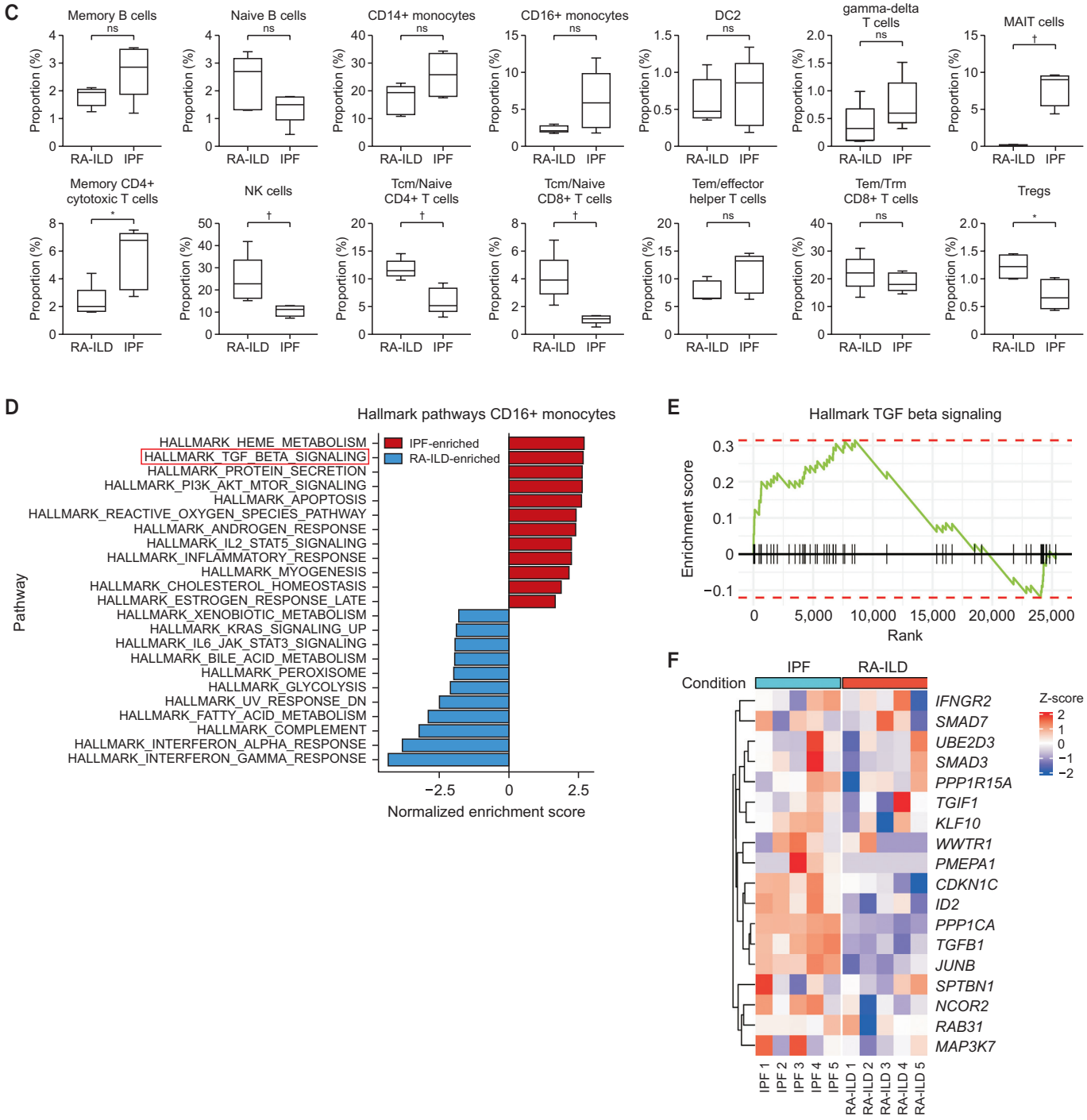

the RA-ILD and IPF groups. Among T/natural killer (NK) cell populations, Tcm/Naive CD8+ T cells, Tcm/Naive CD4+ T cells, and NK cells were significantly decreased in the IPF group. In contrast, mucosal-associated invariant T cells (MAIT) were significantly increased in the IPF group. Additionally, memory $CD4^+$ cytotoxic T cells were significantly increased in the IPF group, whereas regulatory T cells (Tregs) were significantly increased in the RA-ILD group. Consistent with this, NK cells from RA-ILD patients exhibited upregulation of genes associated with inflammation and cytotoxicity, including granzyme B (*GZMB*), granzyme H (*GZMH*), and perforin 1 (*PRF1*). In addition, interferon-related genes such as signal transducer and activator of tran-

scription 1 (*STAT1), STAT3*, interferon regulatory factor 9 (*IRF9*), and interferon-gamma (*IFNG*) expression were also increased, potentially associated with the tissue damage in RA-ILD.

Among myeloid cell subtypes, both CD14+ monocytes and CD16+ monocytes showed a trend toward increased proportions in the IPF group; however, these changes did not reach statistical significance. Given that myeloid populations are known to play a critical role in fibroblast activation and fibrotic remodeling, we next examined differential GEX patterns within myeloid cells. To provide a comprehensive view of transcriptional differences across the immune compartment, we additionally performed differential GEX analysis between RA-ILD and IPF for all other immune cell subsets identified in this study; statistically significant DEGs were detected in every subset examined (Supplementary Table S1). CD16+ monocytes from the IPF group exhibited significant enrichment of the transforming growth factor beta (TGF-β) signaling pathway, which is known to contribute to the development of fibrosis (Figure 2D). In contrast, CD16+ monocytes from the RA-ILD group showed enrichment of both the type I and II interferon response pathways, consistent with the autoimmune milieu characteristic of the RA environment. Notably, this interferon-associated feature mirrored the increased interferon signaling observed in NK cells. These transcriptional differences were further confirmed using running enrichment score plots (Figure 2E). In addition, we examined the leading-edge genes identified from the GSEA results (Figure 2F). This analysis revealed upregulation of fibrosis-related genes such as *TGFB1, SMAD3, SMAD7*, and *TGIF1*, which are key regulators of fibrosis in IPF.

Discussion

In our study, we performed scRNA-seq of PBMCs from patients with RA-ILD and IPF to delineate transcriptomic differences that may underlie their distinct pathogenic mechanisms. Although RA-ILD frequently presents with a UIP pattern similar to IPF, our findings demonstrate that the immunologic and fibrotic pathways involved in these two conditions diverge substantially. In our analysis, IPF was characterized by activation of fibrosis-related pathways, including TGF-β signaling. In contrast, RA-ILD was characterized by an elevation in NK cells with increased inflammatory and cytotoxic GEX, reflecting interferon-driven immune activation rather than a fibrosis-dominant process.

A notable finding was the distinct transcriptional polarization of monocyte subsets between IPF and RA-ILD, rather than a statistically significant difference in their proportions. Although $CD14^+$ and $CD16^+$ monocytes showed a trend toward increased abundance in IPF, their GEX profiles revealed a clear divergence in pathogenic signaling. In IPF, $CD16^+$ monocytes demonstrated strong enrichment of TGF-β–associated pathways. This is consistent with prior work demonstrating that monocyte-driven innate immune activation is a hallmark of IPF pathogenesis, contributing to fibroblast activation and extracellular matrix deposition[21,22]. The upregulation of fibrosis-related genes such as *TGFB1, SMAD3, SMAD7*, and *TGIF1* in IPF further supports the central role of monocyte–fibroblast crosstalk in progressive fibrosis[23]. Moreover, this is consistent with established evidence that TGF-β signaling is a dominant driver of epithelial injury, fibroblast differentiation, and extracellular matrix accumulation in IPF[24,25]. In contrast, $CD16^+$ monocytes in RA-ILD exhibited prominent type I and II interferon response signatures, consistent with the autoimmune-driven inflammatory milieu characteristic of RA-ILD.

Additionally, the significant increase in NK cells observed in RA-ILD, together with enhanced expression of cytotoxic and inflammation mediators (*GZMB*, *GZMH*, *PRF1*) and interferon-related genes (*STAT1*, *STAT3*, *IRF9*, *IFNG*), suggests heightened innate immune activation. This finding is notable, as previous studies have suggested that RA-ILD monocytes share partial transcriptional similarity with IPF monocytes but also display unique inflammatory signatures[21]. Our data extend these observations by demonstrating that, at the single-cell level, RA-ILD is marked by enhanced cytotoxic and inflammatory GEX. These genes are associated with cytotoxic effector function, inflammasome activation, and innate immune sensing, suggesting that innate immune dysregulation may play a more prominent role in RA-ILD than in IPF[26,27]. Interferon-driven transcriptional programs are also well-established features of RA pathogenesis[27,28], supporting the interpretation that NK-cell activation in RA-ILD reflects systemic autoimmune signaling rather than fibrosis-dominant pathways seen in IPF. Collectively, these findings indicate that NK cell-mediated cytotoxic, inflammatory, and interferon responses may represent a disease-specific immunologic axis associated with RA-ILD pathobiology.

While our data demonstrate an elevation of NK cells with cytotoxic and interferon-related GEX in RA-ILD, the functional consequences of these changes should be interpreted with caution. NK cells have been reported to play context-dependent and even opposing roles in fibrosis. On one hand, NK cell-derived cytotoxic and

interferon responses may contribute to tissue inflammation and injury. On the other hand, NK cells can exert anti-fibrotic effects by recognizing and eliminating activated or senescent fibroblasts, thereby limiting fibrotic progression[29]. Notably, reduced NK cell numbers and impaired cytotoxic activity have been reported in IPF lungs, where defective clearance of senescent fibroblasts may facilitate fibrosis[30]. In this context, the relative elevation of NK cells observed in RA-ILD compared with IPF may reflect not only a pro-inflammatory state but also a potential immunomodulatory or reparative response, and our cross-sectional transcriptomic data cannot distinguish between these possibilities. Accordingly, NK cell alterations in RA-ILD are more appropriately regarded as a candidate immunomodulatory feature warranting further functional investigation, rather than a definitively pathogenic mechanism. From a translational perspective, NK cell–related pathways may represent a potential therapeutic target; recent work has shown that restoring NK cell function through NKG2A checkpoint blockade can promote clearance of senescent fibroblasts and resolution of pulmonary fibrosis[31], suggesting that modulation of NK cell activity could be explored as a disease-modifying strategy in fibrotic ILD.

MAIT cells are a specialized, innate-like subset of unconventional T cells found abundantly in human blood, liver, lungs, and mucosa. They play a key role in the immune system by defending against bacterial and fungal infections by recognizing vitamin B2 metabolites presented by MR1 proteins[32]. Interestingly, in this study, MAIT cells were found to be significantly increased in the IPF group compared to the RA-ILD group. Although MAIT cells have not been extensively discussed in the context of pulmonary fibrosis to date, the difference between the two groups suggests that alterations in MAIT cells may represent an immunological feature that has been previously overlooked. Further research on this topic is necessary.

Taken together, our findings support a model in which IPF is characterized primarily by fibroblast-centered profibrotic pathways, whereas RA-ILD is associated with a more complex interplay between NK cell-mediated and interferon-related immune activation. These mechanistic distinctions may help explain differences in disease progression, treatment response, and prognosis between the two conditions. For example, antifibrotic therapies targeting TGF-β signaling may be more effective in IPF, whereas immunomodulatory approaches targeting NK cell activation or cytokine signaling may hold greater promise for RA-ILD.

This study has several limitations. First, the sample size was small, reflecting the rarity of RA-ILD and the challenges of obtaining matched PBMC samples. Second, PBMC-based transcriptomic profiling may not fully capture lung-specific cellular interactions; however, a prior study demonstrated that circulating monocytes and lymphocytes can reflect disease-relevant pathways in ILD[21]. Third, treatment-related confounding is an important limitation that warrants careful consideration. All RA-ILD patients in this study received methotrexate and prednisolone, whereas none of the IPF patients received immunosuppressive therapy. Methotrexate has been shown to substantially alter PBMC immune composition and cytokine profiles in patients with RA[33], and single-cell transcriptomic studies have demonstrated that methotrexate broadly modulates the transcriptional programs of circulating immune cell subsets[34]. Similarly, corticosteroids have been shown to suppress interferon signaling in PBMCs by downregulating STAT1 expression at the single-cell level[35]. Accordingly, the elevated interferon signatures and NK cell activation observed in RA-ILD patients in the present study may reflect, at least in part, the pharmacological effects of these agents rather than intrinsic disease biology. We cannot exclude treatment confounding as a contributing factor within the current cross-sectional design. Future studies incorporating RA patients without ILD receiving comparable immunosuppressive regimens as an additional control group would help disentangle disease-specific from treatment-related transcriptional effects. Fourth, our analysis of cell-cell communication was restricted to soluble and chemokine-mediated interactions inferred from PBMC transcriptomic data, and did not reveal disease-specific signaling patterns between myeloid and lymphoid populations. This may reflect the limited ability of circulating PBMCs to capture contact-dependent, microenvironment-specific interactions that occur within the lung tissue itself. Future studies incorporating lung tissue-based scRNA-seq or spatial transcriptomics would be better suited to characterize immune-myeloid crosstalk in the pathogenesis of RA-ILD and IPF. Fifth, while our differential GEX analysis revealed that several inflammation- and oxidative stress-related genes were significantly upregulated in MAIT cells from IPF patients, the functional and mechanistic significance of these transcriptional changes remains unclear. Our cross-sectional transcriptomic data cannot determine whether these GEX changes reflect a causal contribution of MAIT cells to fibroblast activation and fibrotic remodeling, or whether they represent a secondary, disease-associated bystander phenotype. Furthermore, MAIT cells have not been extensively studied in the context of pulmonary fibrosis,

and functional validation studies, as well as correlation with pathological or spatial transcriptomic findings, will be necessary to clarify the specific role of MAIT cells in IPF pathogenesis. Future studies integrating lung tissue scRNA-seq, serum biomarkers, and longitudinal clinical outcomes are essential to validate and extend our findings.

In our analysis, IPF CD16^{+} monocytes showed upregulated TGF-β signaling. Among RA-ILD patients, baseline levels of NK cells were elevated. In these NK cells, genes related to inflammation and cytotoxicity, such as *GZMB*, *GZMH*, and *PRF1*, were upregulated. Additionally, interferon signaling was increased, potentially associated with the tissue damage in RA-ILD. Our single-cell transcriptomic analysis revealed distinct immunologic and fibrotic mechanisms underlying RA-ILD and IPF. These insights may contribute to improved diagnostic precision and support the development of targeted therapeutic strategies tailored to the unique pathobiology of RA-ILD.

Authors' Contributions

Conceptualization: Kim HJ, Kim BG. Methodology: Kim D, Lee H, Kim HJ, Kim BG. Formal analysis: Kim D, Kim HJ. Data curation: Lee H, Kim SH, Eun Y, Kim BG. Funding acquisition: Lee H, Kim SH, Kim BG. Visualization: Kim D, Kim HJ. Writing - original draft preparation: Kim D, Lee H, Kim BG. Writing - review and editing: all authors. Approval of final manuscript: all authors.

Conflicts of Interest

No potential conflict of interest relevant to this article was reported.

Acknowledgments

The datasets generated and analyzed during the current study are not publicly available due to privacy and confidentiality considerations but may be available from the corresponding author upon reasonable request and subject to institutional approval.

Funding

This study was supported by a 2024 grant from the Korean Academy of Tuberculosis and Respiratory Diseases (KBA24008).

Supplementary Material

Supplementary material can be found in the journal homepage (http://www.e-trd.org).

Supplementary Table S1. Differentially expressed genes between RA-ILD and IPF across 15 immune cell subsets identified by single-cell RNA sequencing of peripheral blood mononuclear cells.

References

1. Choi H, Han K, Jung JH, Park J, Kim BG, Yang B, et al. Impact of rheumatoid arthritis and seropositivity on the risk of non-cystic fibrosis bronchiectasis. Chest 2024;165:1330-40.
2. Kim BG, Lee H, Eun Y, Han K, Jung JH, Choi H, et al. Association between rheumatoid arthritis and interstitial lung disease and impact of serologic status: a large-scale longitudinal study. Sci Rep 2025;15:4885.
3. Kim BG, Yoon S, Lee SY, Kim EG, Kim JO, Kim JS, et al. Multi-ancestry causal association between rheumatoid arthritis and interstitial lung disease: a bidirectional two-sample mendelian randomization study. J Clin Med 2024;13:6080.
4. Bongartz T, Nannini C, Medina-Velasquez YF, Achenbach SJ, Crowson CS, Ryu JH, et al. Incidence and mortality of interstitial lung disease in rheumatoid arthritis: a population-based study. Arthritis Rheum 2010;62:1583-91.
5. Hyldgaard C, Ellingsen T, Hilberg O, Bendstrup E. Rheumatoid arthritis-associated interstitial lung disease: clinical characteristics and predictors of mortality. Respiration 2019;98:455-60.
6. Shaw M, Collins BF, Ho LA, Raghu G. Rheumatoid arthritis-associated lung disease. Eur Respir Rev 2015;24:1-16.
7. Doyle TJ, Dellaripa PF, Batra K, Frits ML, Iannaccone CK, Hatabu H, et al. Functional impact of a spectrum of interstitial lung abnormalities in rheumatoid arthritis. Chest 2014;146:41-50.
8. Raimundo K, Solomon JJ, Olson AL, Kong AM, Cole AL, Fischer A, et al. Rheumatoid arthritis-interstitial lung disease in the United States: prevalence, incidence, and healthcare costs and mortality. J Rheumatol 2019;46:360-9.
9. Hu F, Zhang W, Shi L, Liu X, Jia Y, Xu L, et al. Impaired CD27+IgD+ B cells with altered gene signature in rheumatoid arthritis. Front Immunol 2018;9:626.
10. Li C, Chu T, Zhang Z, Zhang Y. Single cell RNA-seq analysis identifies differentially expressed genes of Treg cell in early treatment-naive rheumatoid arthritis by arsenic trioxide. Front Pharmacol 2021;12:656124.
11. Lu DR, McDavid AN, Kongpachith S, Lingampalli N, Glan-

ville J, Ju CH, et al. T cell-dependent affinity maturation and innate immune pathways differentially drive autoreactive B cell responses in rheumatoid arthritis. Arthritis Rheumatol 2018;70:1732-44.
12. Mizoguchi F, Slowikowski K, Wei K, Marshall JL, Rao DA, Chang SK, et al. Functionally distinct disease-associated fibroblast subsets in rheumatoid arthritis. Nat Commun 2018;9:789.
13. Orange DE, Yao V, Sawicka K, Fak J, Frank MO, Parveen S, et al. RNA identification of PRIME cells predicting rheumatoid arthritis flares. N Engl J Med 2020;383:218-28.
14. Stephenson W, Donlin LT, Butler A, Rozo C, Bracken B, Rashidfarrokhi A, et al. Single-cell RNA-seq of rheumatoid arthritis synovial tissue using low-cost microfluidic instrumentation. Nat Commun 2018;9:791.
15. Zhang F, Wei K, Slowikowski K, Fonseka CY, Rao DA, Kelly S, et al. Defining inflammatory cell states in rheumatoid arthritis joint synovial tissues by integrating single-cell transcriptomics and mass cytometry. Nat Immunol 2019;20:928-42.
16. Laria A, Lurati AM, Zizzo G, Zaccara E, Mazzocchi D, Re KA, et al. Interstitial lung disease in rheumatoid arthritis: a practical review. Front Med (Lausanne) 2022;9:837133.
17. Matson S, Lee J, Eickelberg O. Two sides of the same coin? A review of the similarities and differences between idiopathic pulmonary fibrosis and rheumatoid arthritis-associated interstitial lung disease. Eur Respir J 2021;57:2002533.
18. Kim BG, Kim Y, Lee SH, Lee S, Choi M, Lee B, et al. T-cell immune dysfunction and progression to severe COVID-19 in asthma revealed by single-cell RNA sequencing. Tuberc Respir Dis (Seoul) 2026;89:38-54.
19. Young MD, Behjati S. SoupX removes ambient RNA contamination from droplet-based single-cell RNA sequencing data. Gigascience 2020;9:giaa151.
20. Germain PL, Lun A, Garcia Meixide C, Macnair W, Robinson MD. Doublet identification in single-cell sequencing data using scDblFinder. F1000Res 2022;10:979.
21. Poole JA, Schwab A, Thiele GM, England BR, Nelson AJ, Gleason A, et al. Unique transcriptomic profile of peripheral blood monocytes in rheumatoid arthritis-associated interstitial lung disease. Rheumatology (Oxford) 2025;64:SI37-46.
22. Lema D, Kosak Lopez E, Lam J, Tskhakaia I, Gonzalez Moret Y, Abdollahi S. The role of monocytes in the natural history of idiopathic pulmonary fibrosis: a systematic literature review. Int J Mol Sci 2025;26:6538.
23. Tsitoura E, Trachalaki A, Vasarmidi E, Mastrodemou S, Margaritopoulos GA, Kokosi M, et al. Collagen 1a1 expression by airway macrophages increases in fibrotic ILDs and is associated with FVC decline and increased mortality. Front Immunol 2021;12:645548.
24. Chen F, Lyu L, Xing C, Chen Y, Hu S, Wang M, et al. The pivotal role of TGF-β/Smad pathway in fibrosis pathogenesis and treatment. Front Oncol 2025;15:1649179.
25. Massague J, Sheppard D. TGF-β signaling in health and disease. Cell 2023;186:4007-37.
26. Chin A, Small A, Wong SW, Wechalekar MD. T cell dysregulation in rheumatoid arthritis: from genetic susceptibility to established disease. Curr Rheumatol Rep 2025;27:14.
27. Xu J, Li C, Zhao J, Mu R. Shared immunological pathways in rheumatoid arthritis-related interstitial lung disease. Front Immunol 2025;16:1630729.
28. van der Pouw Kraan TC, Wijbrandts CA, van Baarsen LG, Voskuyl AE, Rustenburg F, Baggen JM, et al. Rheumatoid arthritis subtypes identified by genomic profiling of peripheral blood cells: assignment of a type I interferon signature in a subpopulation of patients. Ann Rheum Dis 2007;66:1008-14.
29. Yang M, Vanderwert E, Kimchi ET, Staveley-O'Carroll KF, Li G. The important roles of natural killer cells in liver fibrosis. Biomedicines 2023;11:1391.
30. Cruz T, Jia M, Sembrat J, Tabib T, Agostino N, Bruno TC, et al. Reduced proportion and activity of natural killer cells in the lung of patients with idiopathic pulmonary fibrosis. Am J Respir Crit Care Med 2021;204:608-10.
31. Merkt W, Rodon L, Deicher FS, Freitag M, Claus M, Lister R, et al. Natural killer cell immunotherapy reverses lung fibrosis by eliminating senescent fibroblasts. Sci Transl Med 2026;18:eadq5442.
32. Hinks TS. Mucosal-associated invariant T cells in autoimmunity, immune-mediated diseases and airways disease. Immunology 2016;148:1-12.
33. Kremer JM, Lawrence DA, Hamilton R, McInnes IB. Long-term study of the impact of methotrexate on serum cytokines and lymphocyte subsets in patients with active rheumatoid arthritis: correlation with pharmacokinetic measures. RMD Open 2016;2:e000287.
34. Yang Z, Liang Q, Liang H, Chen W, Li C, Xiao Y, et al. Single-cell RNA transcriptomic and plasma lipidomic reveal the potential mechanisms of a methotrexate-based therapy against rheumatoid arthritis. Phytomedicine 2023;115:154816.
35. Jeong HW, Lee JS, Ko JH, Hong S, Oh ST, Choi S, et al. Corticosteroids reduce pathologic interferon responses by downregulating STAT1 in patients with high-risk COVID-19. Exp Mol Med 2023;55:653-64.